ELSEVIER

Journal of Hazardous Materials 142 (2007) 68–76

Journal of Hazardous Materials

www.elsevier.com/locate/jhazmat

Removal of basic yellow dye from aqueous solution by sorption on green alga *Caulerpa scalpelliformis*

Rathinam Aravindhan, Jonnalagadda Raghava Rao *, Balachandran Unni Nair

Chemical Laboratory, Central Leather Research Institute, Adyar, Chennai 600020, India

Received 23 May 2006; received in revised form 24 July 2006; accepted 26 July 2006
Available online 31 July 2006

Abstract

Dynamic batch experiments were carried out for the biosorption of basic yellow dye on to the green macroalgae *Caulerpa scalpelliformis*. The factors affecting the sorption process such as the initial concentration of the dye and pH of the solution, the adsorbent dosage and the time of contact were studied. The sorption kinetics followed pseudo-second order kinetic model. The *Caulerpa* species exhibited a maximum uptake of 27 mg of dye per gram of seaweed. The Boyd's plot confirmed the external mass transfer as the rate-limiting step. The average effective diffusion coefficient was found to be 2.47×10^{-4} cm^2/s. Sorption equilibrium studies demonstrated that the biosorption followed Freundlich isotherm model, which implies a heterogeneous sorption phenomenon. Various thermodynamic parameters such as enthalpy of sorption ΔH°, free energy change ΔG° and entropy ΔS° were estimated. The negative value of ΔH° and negative values of ΔG° show the sorption process is exothermic and spontaneous. The negative value of entropy ΔS° shows the decreased randomness at the solid–liquid interface during the sorption of dyes onto green seaweed.

Keywords: Basic yellow dye; Biosorption; Diffusion coefficient; Equilibrium isotherm; Green seaweed; Macroalgae

1. Introduction

Pollution control is one of the prime concerns of society today. Untreated or partially treated wastewaters and industrial effluents into natural ecosystems pose a serious problem to the environment. Among the industrial wastewaters, the removal of color from dye bearing effluents is one of the major problems due to the difficulty in treating such wastewaters by conventional treatment methods. This is because synthetic dyes have a complex aromatic molecular structure, which makes them more stable and difficult to biodegrade [1]. Although number of processes like flocculation, chemical coagulation, precipitation, ozonation and adsorption has been employed for the treatment of dye bearing wastewaters, they possess inherent limitations such as high cost, formation of hazardous by-products and intensive energy requirements [2]. Biological processes such as bioaccumulation and biodegradation have been proposed as having potential application in removal of dyes from dye bearing wastewater [3,4].

Biosorption passive uptake of pollutants from aqueous solutions by the use of non-growing or non-living microbial mass, thus allowing the recovery or environmentally acceptable disposal of the pollutants, could also be considered [5–8]. The main attractions of biosorption are high selectivity and efficiency, cost effectiveness and good removal performance. Raw materials, which are either abundant or wastes from other industrial operations, can be used as biosorbents, presenting performances often comparable with those of ion exchange resins. The use of dead cells in biosorption is most advantageous for wastewater treatment in that, the dead organisms are not affected by toxic wastes, do not require a continuous supply of nutrients and can be regenerated and reused for many cycles. Dead cells may be stored or used for extended periods at room temperature without putrefaction. Biological materials such as chitin, chitosan, peat, yeasts, fungi or bacterial biomass are used as chelating and complexing sorbents in order to concentrate and remove dyes from solutions [9–14]. However, these low cost adsorbents have generally low adsorption capacities, leading to utilization of large amounts of adsorbents.

Algae have been found to be potential, suitable biosorbent because of their fast and easy growth and their wide availability. The special surface properties of algae, bacteria and fungi

* Corresponding author. Tel.: +91 44 24411630; fax: +91 44 24911589.
E-mail address: clrichem@mailcity.com (J.R. Rao).

0304-3894/$ – see front matter © 2006 Elsevier B.V. All rights reserved.
doi:10.1016/j.jhazmat.2006.07.058

enable them to adsorb different kinds of metallic and organic pollutants from solutions. Algal cell wall offers a host of functional groups including amino, carboxyl, sulfate, phosphate and imidazoles associated with polysaccharides alginic acid and proteins for binding various pollutants [15]. Different micro/macroalgal species have been proved to be effective biosorbent for the treatment of wastewater. But almost all the studies have been focused only on the removal of metal cations from wastewaters [16,17]. Even though thousands of algal species are known, only a few of them have been investigated for their organic pollution control ability and subsequent use for wastewater treatment. In the present investigation, the biomass of green seaweed has been used as a biosorbent and its capacity to remove basic dye (cationic dye) has been evaluated.

2. Materials and methods

Beach-dried green seaweed *Caulerpa scalpelliformis* was procured from Central Salt and Marine Chemicals Research Institute (CSMCRI), Mandapam Camp, Ramnad District, India. The beach-dried seaweeds were washed with distilled water, shade dried and stored in an airtight pack at room temperature ($28 \pm 2\,^{\circ}C$). The moisture content of the dried seaweed was $5 \pm 1\%$ (w/w). The dye used in all the experiments was Sandocryl golden yellow C-2G,[1] a cationic dye, obtained from Clariant India Ltd. The synthetic dye solution was prepared by dissolving weighed amount of the dye in 1 L of distilled water. Basic dyes fall within the class of polymethine dyes. As such they are cationic polymethines; because ionization in solution they possess an overall positive charge and are therefore widely used to bind to negatively charged substrates [18]. All other reagents used were of analytical grade. Distilled water was used throughout the experiments.

2.1. Characterization of biosorbent

The acidic and ion exchange properties of the green seaweed were determined in order to study the nature and capacity of the biosorbent. The potentiometric titrations of the green seaweed were performed with 40 mL of 0.05 M KNO_3 as background electrolyte. The pH of the seaweed suspension was adjusted to ca. 2.00 with known amount of 0.127 N HCl The stirred suspension was allowed to equilibrate until the pH was stable before the titrations started. The suspension was then titrated with standard NaOH solution. The pH of the suspension was measured after titrant addition by using a pH-meter. After each addition of titrant the system was allowed to equilibrate until a stable reading was obtained. The number of carboxyl groups per gram of alga $[COOH]_{total}$ (mmol g^{-1}) was calculated by estimation of the position of inflection point (V_{eq}) in the resulting titration curve, using the following equation:

$$[COOH]_{total} = \frac{V_{eq}[NaOH]}{S} \quad (1)$$

[1] Commercial dye used for dyeing of leather. Structure and CI number of the dye are unknown.

The FT-IR spectra of untreated, pretreated, and chromium treated seaweed were obtained using the KBr disk technique. The seaweed was ground in a mortar for 5 min after drying it for a period of 2 h at 80 °C. Dilution and homogenization to 0.01% (w/w) with KBr (spectroscopic grade) were carried out with additional grinding. The disks were pressed in a hydraulic KBr press. The transmission FT-IR spectra were then recorded between 400 and 4000 cm^{-1} using a Perkin-Elmer Spectrum RX I FT-IR system.

2.2. Biosorption experiments

The effect of pH and adorbent dosage on uptake capacity of the seaweed for the dye was obtained by agitating 5 g/L of seaweed in a series of bottles, containing 50 mL of dye solution of initial concentration 150 mg/L at different solution pH ranging from 3.0 to 8.0 and with weighed amount of green seaweed ranging from 3 to 10 g/L, respectively. The effect of initial concentration of dye on the equilibrium uptake by green seaweed was estimated by contacting 5 g/L of seaweed with 50 mL of dye solution of different initial concentrations ranging from 25 to 150 mg/L. The experiments were carried out in a mechanical agitator maintained at room temperature for a period of 4 h. The concentration of the dye in the solution before and after adsorption was determined by measuring the absorbance of the solution at 438 nm using Perkin-Elmer Lambda 35 UV–vis spectrophotometer.

2.3. Adsorption kinetics and equilibrium studies

Adsorption kinetic experiments were carried out by agitating 100 ml of dye solution of known initial dye concentration with 5 g/L of seaweed at room temperature ($30 \pm 1\,^{\circ}C$) at a pH of 6.0 ± 0.1 at a constant agitation speed of 75 strokes/min. Similarly the equilibrium experiments were carried out by contacting 3–10 g/L of seaweed with 50 mL of dye solution of different initial dye concentrations (25, 50, 100 and 150 mg/L). The samples were agitated in water bath at a constant speed of 75 strokes/min for 4 h at room temperature. The concentration of the dye in the solution before and after sorption was determined using Perkin-Elmer Lambda 35 UV–vis spectrophotometer.

The amount of dye adsorbed on to the seaweed at equilibrium was calculated from the mass balance of the equation as given below:

$$q_e = (C_0 - C_e)\frac{V}{W} \quad (2)$$

where C_0 and C_e are the initial and equilibrium concentration of dye solution (mg/L), respectively, q_e is the equilibrium dye concentration on seaweed (mg/g), V the volume of the dye solution (L) and W is the mass of the seaweed used (g).

3. Results and discussion

Adsorption of basic yellow dye on to green seaweed was systematically investigated by studying the effect of various

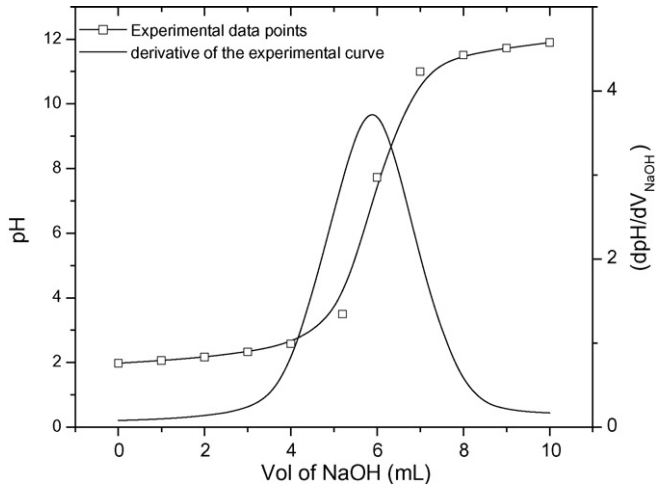

Fig. 1. Acid–base potentiometric titration of the acid-treated *Caulerpa scalpelliformis* sample.

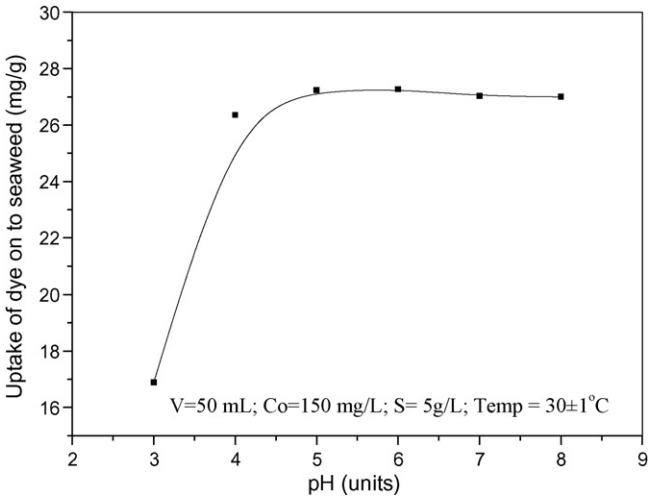

Fig. 3. Effect of pH.

parameters such as pH, adsorbent dosage and initial dye concentration.

3.1. Characterization of seaweed

The total amount of proton binding sites in green seaweed was estimated by a potentiometric titration of the seaweed. The potentiometric titration data along with the first derivative plot are presented in Fig. 1. The total organic acidity ($[COOH]_{total}$) was 2.89 mmol g^{-1}. The FT-IR spectra (Fig. 2) of the green seaweed in the range of 400–4000 cm^{-1} were taken in order to obtain information on the nature of cell wall and dye interaction. It exhibits absorption bands at 3430, 2924, 1654 and 1030 cm^{-1}, which indicate the presence of –OH, –COOH, C=O and C–O groups, respectively.

3.2. Effect of pH

Adsorpt of dye by the green seaweed is dependent upon the pH of the initial dye solution. The effect of initial pH of the dye solution on the adsorption capacity of the seaweed is presented in Fig. 3. It is observed that uptake increases from 17 to 27 mg/g for an increase in pH from 3.0 to 8.0. Several reasons may be attributed to the adsorption of dye by the seaweed relative to pH. The surface of the seaweed contains large number of reactive sites. At lower pH, the surface of the seaweed gets positively charged thus making the H^+ ions compete effectively with dye cations causing decrease in the amount of dye adsorbed (mg/g). At higher pH, the surface of the seaweed gets negatively charged, which enhances the interaction of positively charged dye cations with the surface of seaweed through the electrostatic forces of attraction [19]. All the experiments are conducted at a pH of 6.0 ± 0.1, for the % uptake was higher at this pH and equilibrium has been reached thereafter.

3.3. Effect of seaweed loading

Fig. 4 shows the plot of amount of dye adsorbed (q_e) and the % dye removal against the quantity of seaweed (g) employed. From the figure it is observed that removal efficiency (%) increases from 81 to 95% with increase in the adsorbent loading from 3 to 10 g/L. This can be attributed to an increase in surface area of the biosorbent, which in turn increases the binding sites. At higher seaweed dosage, there is a very fast adsorption on to the adsor-

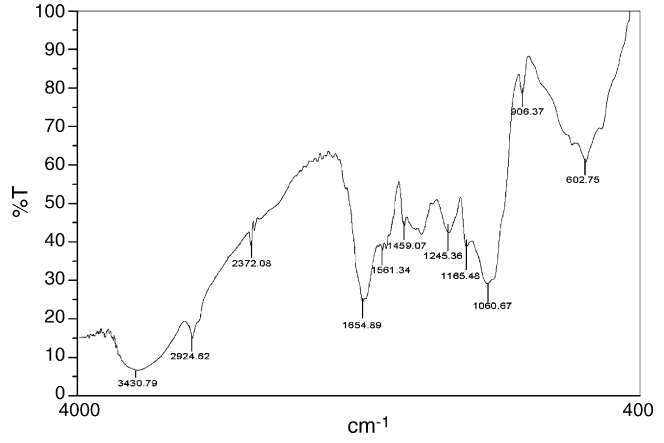

Fig. 2. FT-IR spectrum of green seaweed *C. scalpelliformis*.

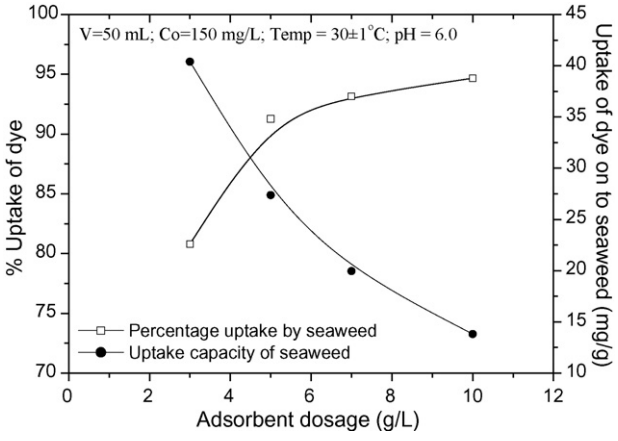

Fig. 4. Effect of initial adsorbent dosage.

bent surface that leads to improved uptake of the dye. However, with increasing seaweed load, the quantity of dye adsorbed on to the unit weight of seaweed gets reduced, thus causing a decrease in q_e value with increasing seaweed loading. This may be due to complex interactions of several factors including availability of solute, electrostatic interactions and interference between binding sites, etc. The important factors being at high sorbent dosages the available dye molecules are insufficient to cover all the exchangeable sites on the biosorbent, usually resulting in low dye uptake.

3.4. Effect of initial dye concentration and time

A higher initial concentration provides an important driving force to overcome all resistances of the dye between the aqueous and solid phases, thus increasing the uptake. In addition, increasing the initial dye concentration increases the number of collisions between dye ions and the seaweeds, which enhances the adsorption process. Fig. 5 shows the plot the quantities of dye adsorbed (q_t) versus time t at different dye concentrations, where q_t represents the amount of dye adsorbed at any time t. From the figure it can be observed that the amount of dye adsorbed varies with varying initial dye concentration and increases with increase in initial dye concentration. The amount of dye adsorbed increases from 4.7 to 27 mg/g for an increase in initial dye concentration from 25 to 150 mg/L. The effect of initial dye concentration on the biosorption capacity has been found to be of considerable significance for the basic dye used.

3.5. Effect of temperature

The effect of temperature on the sorption capacity of green seaweed was studied at 20, 30, 40, 50 and 60 °C and the results were shown in Fig. 6. The results show that the sorption capacity decreased from 28 to 23 mg/g with temperature increase from 20 to 60 °C. The equilibrium uptake of the cationic yellow dye decreased with increasing temperature suggesting that biosorption between *C. scalpelliformis* and cationic yellow dye was an exothermic process and the mechanism was mainly physical adsorption, dominant at lower temperatures.

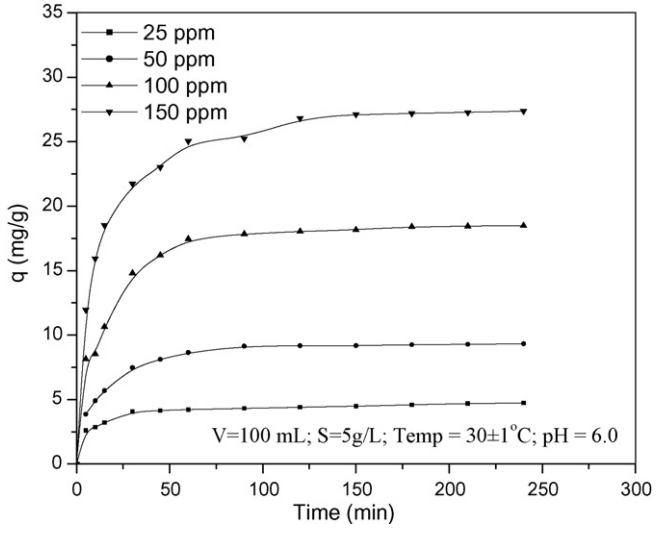

Fig. 5. Effect of initial concentration.

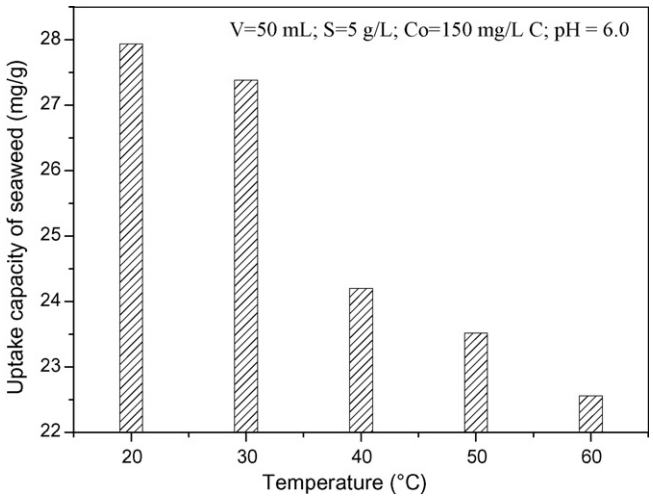

Fig. 6. Effect of temperature.

3.6. Kinetics of adsorption process

The principle behind the adsorption kinetics involves the search for a best model that well represents the experimental data. Several kinetic models are available to understand the behavior of the adsorbent and also to examine the controlling mechanism of the adsorption process and to test the experimental data. In the present investigation, the adsorption data were analyzed using two simplest kinetic models, the pseudo-first order and pseudo-second order kinetic models.

The rate constant of adsorption is determined from the following pseudo-first order rate expression given by Lagergren [20]:

$$\log(q_e - q) = \log q_e - \frac{k_1}{2.303} t \tag{3}$$

where q_e is the amount of dye adsorbed (mg/g) at equilibrium, q the amount of dye adsorbed (mg/g) at time t (min) and k_1 is the pseudo-first order rate constant of adsorption.

A straight line of $\log(q_e - q)$ versus t suggests the applicability of this kinetic model. In order to fit Eq. (3) to experimental data, the equilibrium adsorption capacity, q_e must be known. In many cases q_e is unknown and as adsorption tends to become immeasurably slow, the amount sorbed is still significantly smaller than the equilibrium amount. For this reason it is necessary to obtain the real equilibrium adsorption capacity, q_e, by extrapolating the experimental data to $t = \infty$ or by using a trial and error method. Furthermore, in most cases the first order equation of Lagergren does not fit well for the whole range of contact time and is generally applicable over the initial 20–30 min of the adsorption process. The first order rate constant (k_1) and q_e were determined from the slopes and intercepts of plots of $\log(q_e - q)$ versus t at different adsorbent dosages.

Table 1
Rate constants for kinetic models at various initial concentrations

Initial concentration (mg/L)	$q_{e(exp)}$ (mg/g)	Pseudo-first order rate constants			Pseudo-second order rate constants		
		k_1 (min^{-1})	$q_{e(cal)}$ (mg/g)	R^2	k_2 (g/mg min)	$q_{e(cal)}$ (mg/g)	R^2
25	4.72	0.0018	1.940	0.913	0.028479	4.799	0.999
50	9.32	0.0237	4.075	0.952	0.012337	9.686	0.999
100	18.48	0.0266	9.672	0.972	0.005713	19.283	0.999
150	27.38	0.0264	15.118	0.963	0.004174	28.385	0.999

The kinetics of adsorption can also be described by pseudo-second order equation and it is given by [21]:

$$\frac{t}{q} = \frac{1}{k_2 q_e^2} + \frac{1}{q_e} t \quad (4)$$

The second order rate constant (k_2) and q_e were determined from the slope and intercepts of the plots obtained by plotting t/q_t versus time t. The value of q determined experimentally $q_{e(exp)}$, calculated $q_{e(cal)}$, correlation coefficient together with the adsorption rates k_1 and k_2 are shown in Table 1.

The correlation coefficients for the first order kinetic model were determined and compared with that of second order kinetic model. It is seen that the correlation coefficient of first order kinetic are lower than in the case of second order kinetic model (Table 1). This shows that kinetics of dye adsorption by green seaweed are better described by pseudo-second order kinetic model rather than pseudo-first order. The linearity of the plot (figure not shown) also shows the applicability of the pseudo-second order kinetic model, which has average regression coefficient of R^2 0.997. Also, $q_{e(cal)}$ using pseudo-second order kinetic model is in par with $q_{e(exp)}$ which has been obtained experimentally.

3.7. Biosorption mechanisms

Prediction of the rate-limiting step is an important factor to be considered in adsorption process [22]. For solid–liquid adsorption process, either external mass transfer or intraparticle diffusion or both usually characterize the solute transfer process. The overall rate of adsorption will be controlled by the slowest step, which would be either film diffusion or pore diffusion. The external mass transfer is characterized by the initial solute uptake and can be calculated from the slope of plot between C/C_0 versus time [23,24]. The intraparticle diffusion coefficient for the adsorption of the basic yellow dye has been calculated from the slope of the plot of square root of time (min$^{0.5}$) versus amount of dye adsorbed (mg/g) (Fig. 7). It has been shown earlier that the plot between q versus $t^{0.5}$ represents multi-linearity, characterizes two or more steps involved in adsorption process [25]. From the figure, it is clear that at all initial dye concentrations, the adsorption process follows two phases. It is observed that an initial linear portion ended with a smooth curve followed by second linear portion. The two phases in the intraparticle diffusion plot suggests that the adsorption process proceeds by surface adsorption and the intraparticle diffusion. The initial curved portion of the plot indicates boundary layer effect while the second linear portion is due to intraparticle or pore diffusion. The slope of second linear portion of the plot has been defined as the intraparticle diffusion parameter k_i (mg/g min). The calculated intraparticle diffusion coefficient k_i values at different initial dye concentrations are shown in Table 2. The biphasic nature of intraparticle diffusion plot confirms the presence of both film and pore diffusion. In order to predict the actual slow step involved, the kinetic data are further analyzed using Boyd kinetic expression which is given by [26]:

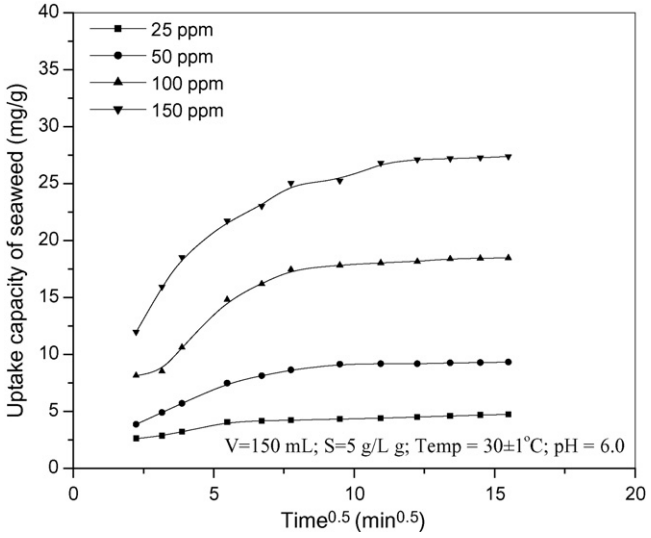

Fig. 7. Intraparticle diffusion.

$$F = 1 - \frac{6}{\pi^2}\exp(-B_t) \quad (5)$$

and

$$F = \frac{q_t}{q_e} \quad (6)$$

where q_e is the amount of dye adsorbed at infinite time (mg/g), q_t the amount of dye adsorbed at any time t (min), F the fraction of

Table 2
Intraparticle diffusion constant and effective diffusivity at different initial dye concentration

C_0 (mg/L)	k_i (mg/g min)	D_i ($\times 10^{-4}$ cm^2/s)
25	0.1428	3.98
50	0.3725	3.38
100	0.7646	1.52
150	1.0093	9.75
Average		2.47

solute adsorbed at any time t and B_t is a mathematical function of F.

Rearranging Eq. (5):

$$1 - F = \frac{6}{\pi^2}\exp(-B_t) \tag{7}$$

or

$$B_t = -0.4977 - \ln(1 - F) \tag{8}$$

Eq. (8) is used to calculate B_t values at different time t. The linearity of the plot of B_t versus time is used to distinguish whether external and intraparticle transport controls the adsorption rate. It is observed that the relation between B_t and t is linear (average $R^2 = 0.950$) at all dye concentrations but does not pass through origin, confirming that surface diffusion is the rate-limiting step [27]. The calculated B values are used to calculate the effective diffusion coefficient, D_i (cm^2/s) using the relation:

$$B = \pi^2 \frac{D_i}{r^2} \tag{9}$$

where r represents the radius of the particle calculated by sieve analysis and by assuming as spherical particles. The calculated D_i values at different initial dye concentrations are provided in Table 2. The average D_i values are estimated to be 2.47×10^{-4} cm^2/s.

3.8. Equilibrium adsorption studies

Adsorption equilibrium is established when the amount of solute being adsorbed on to the adsorbent is equal to the amount being desorbed. At this point, the equilibrium solution concentration remains constant. By plotting solid phase concentration against liquid phase concentration graphically, it is possible to depict the equilibrium adsorption isotherm. There are many theories relating to adsorption equilibrium. In the present investigation the equilibrium data are analyzed using the Langmuir and Freundlich isotherm expression given by Eqs. (10) and (11), respectively [28,29].

The Langmuir isotherm theory assumes monolayer coverage of adsorbate over a homogeneous adsorbent surface, i.e. the surface consists of identical sites, equally available for adsorption and with equal energies of adsorption. Therefore, at equilibrium, a saturation point is reached where no further adsorption can occur. Adsorption is assumed to take place at specific homogeneous sites with the adsorbent and once a dye molecule occupies a site, no further adsorption can take place at the site.

Langmuir constants q_0 and b can be determined from the linear plot of C_e/q_e versus C_e, which has a slope of $1/q_0$ and an intercept of $1/q_0 b$. The linear form of Langmuir equation is given by:

$$\frac{C_e}{q_e} = \frac{1}{q_0 b} + \frac{C_e}{q_0} \tag{10}$$

The experimental dye uptake values obtained have also been analyzed using Freundlich equation. In Freundlich adsorption isotherm, the model assumes that the adsorbent consists of a heterogeneous surface composed of different classes of adsorption sites. The Freundlich constants n and k are obtained from the linear regression analysis of the equation:

$$\log q_e = \log K_f + \frac{1}{n}\log C_e \tag{11}$$

where q_e is the maximum uptake capacity and C_e is the equilibrium concentration. Plot of $\log q_e$ versus $\log C_e$ should give a straight line with a slope of $1/n$ and intercept of $\log K_f$.

A linear relation was observed among the plotted parameters with the R^2 value of 0.710 and 0.930 for Langmuir and Freundlich isotherms, respectively (figure not shown). The predicted Freundlich and Langmuir isotherm equation at 30 °C, for basic yellow dye on to green seaweed, useful for design calculations are given respectively by the following equations:

$$q_e = 3.19 C_e^{0.775} \tag{12}$$

$$q_e = \frac{2.33 C_e}{1 + 0.0212 C_e} \tag{13}$$

The Freundlich and Langmuir curve for the adsorption process have been generated using the Eqs. (12) and (13), and presented in Fig. 8. The K_f and $1/n$ values obtained from the Freundlich isotherm were found to be 3.193 and 0.775, respectively, with an R^2 value of 0.930. The shape of the isotherm, R^2 values and the heterogeneity factor ($1/n$) seem to support a Freundlich model for adsorption.

3.9. Thermodynamic parameters

Based on fundamental thermodynamic concept, it is assumed that in an isolated system, energy cannot be gained or lost and the entropy change is the only driving force. In environmental engineering practice, both energy and entropy factors must be considered in order to determine which process will occur spontaneously. The Gibbs free energy change, ΔG°, is the funda-

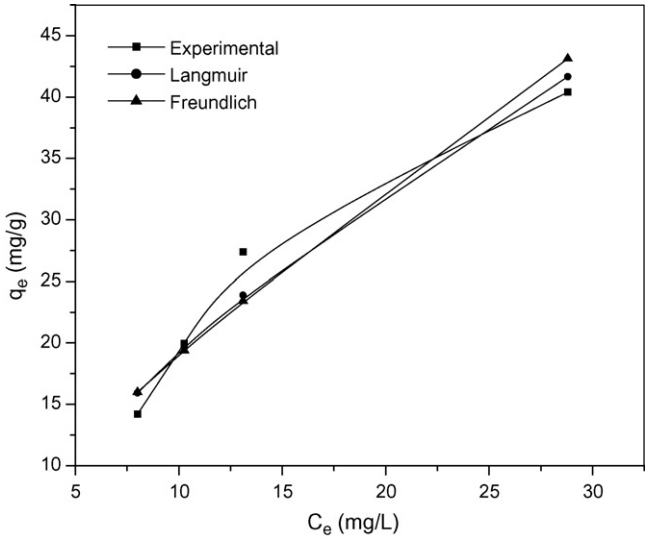

Fig. 8. Comparison of experimental and model fits of Langmuir and Freundlich isotherms for the adsorption of cationic yellow dye onto green seaweed biomass.

Table 3
Thermodynamic parameters for adsorption of basic yellow dye on green seaweed

Concentration of dye (mg/L)	ΔH° (kJ/mol)	ΔS° (kJ/mol K)	$-\Delta G^\circ$ (kJ/mol)				
			293 K	303 K	313 K	323 K	333 K
150	−3.306	−0.091	6.334	5.422	4.510	3.598	2.686

mental criterion of spontaneity. Reactions occur spontaneously at a given temperature if ΔG° is a negative quantity.

The thermodynamic parameters such as changes in standard free energy (ΔG°), enthalpy (ΔH°) and entropy (ΔS°), were determined by using the following equations:

$$K_d = \frac{C_a}{C_e} \tag{14}$$

$$\Delta G^\circ = \Delta H^\circ - T\,\Delta S^\circ \tag{15}$$

$$\ln K_d = \frac{\Delta S^\circ}{R} - \frac{\Delta H^\circ}{RT} \tag{16}$$

where K_d is the distribution coefficient for the adsorption, C_a the amount of dye (mg) adsorbed on the adsorbent per liter of the solution at equilibrium and C_e is the equilibrium concentration (mg/L) of the dye in the solution. T is the solution temperature (K) and R is the gas constant. ΔH° and ΔS° were calculated from the slope and intercept of van't Hoff plots of $\ln K_d$ versus $1/T$. The results are listed in Table 3. Distribution coefficient (K_d) indicates the capability of the seaweed to retain dye molecules and also the extent of its movement in a solution phase [30]. According to Fontes and Gomes [31], K_d is a useful parameter for comparing the adsorptive capacities of different adsorbent materials for any particular ion, when measured under same experimental conditions.

Generally, the absolute magnitude of the change in free energy for physisorption is between −20 and 0 kJ/mol and chemisorption has a range of −80 to −400 kJ/mol [32]. The change in free energy for adsorption of dye onto green seaweed is −5.42 kJ/mol at 30 °C, with an initial concentration of 150 mg/L. Hence, this process can be considered as physisorption. The negative values of ΔG° indicate that the adsorption of dye on the seaweed is spontaneous. It can also be noted that the change in free energy decreases with increase in temperature. The negative value of change in enthalpy (ΔH°) shows that the adsorption is exothermic in nature. Negative value of change in entropy (ΔS°) reflects the decreased randomness at the solid/solution interface during the adsorption of dye on seaweed. This is a direct consequence of: (i) opening up of seaweed structure, (ii) enhancing the mobility and extent of penetration within the seaweed, and (iii) overcoming the activation energy barrier and enhancing the rate of intraparticle diffusion.

3.10. Designing batch adsorption from isotherm data

Empirical design procedures based on sorption equilibrium conditions are the most common method for predicting the adsorber size and performance. Previously, sorption isotherm relations have been used to predict the design of single-stage batch-sorption systems [33]. A schematic diagram is shown in Fig. 9 where the effluent contains V (L) of water and an initial dye concentration C_0, which is to be reduced to C_1 during the adsorption process. The amount of adsorbent used is W (g) and the dye concentration on the seaweed changes from Q_0 to Q_1. At time $t = 0$, $Q_0 = 0$ and as time proceeds the mass balance equates the dye removed from the liquid to that taken up by the sorbent. The mass balance that equates the dye removed from the liquid effluent to that accumulated by the solid is:

$$V(C_0 - C_1) = W(Q_1 - Q_0) = WQ_1 \tag{17}$$

Under equilibrium conditions:

$$C_1 \to C_e \quad \text{and} \quad Q_1 \to Q_e \tag{18}$$

Since the sorption isotherm studies confirm that the equilibrium data for basic yellow dye onto seaweed fitted well in a Freundlich isotherm, Freundlich isotherm equation can be used for Q_1 in Eq. (17) for batch adsorber design. Eq. (19) can be rearranged as:

$$\frac{W}{V} = \frac{C_0 - C_1}{Q_e} = \frac{C_0 - C_e}{K_f C_e^{1/n}} \tag{19}$$

Fig. 10 shows the plot between the predicted amounts of green seaweed required to remove basic yellow dye solutions of initial concentrations 150 mg/L for 50, 75, and 90% color removal at different solution volumes (1–10 L). For example, amounts of green seaweed required for the 75% removal of basic yellow dye solution of concentration 150 mg/L was 4.25, 10.62, 16.99, and 21.24 g for dye solution volumes of 2, 5, 6 and 10 L, respectively.

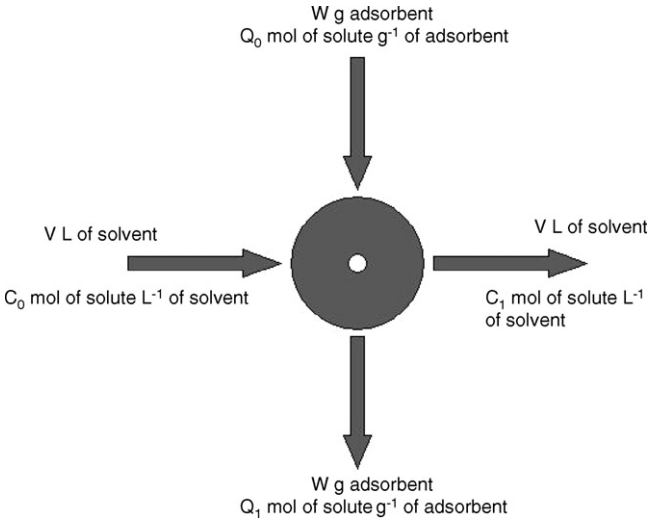

Fig. 9. Single-stage batch-adsorber design.

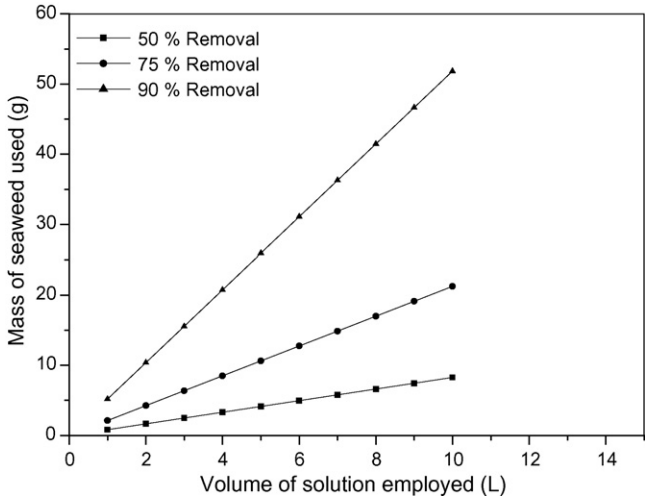

Fig. 10. Adsorbent mass (M) against volume of solution treated (L).

4. Conclusion

The present investigation reports kinetic and equilibrium studies on biosorption of cationic yellow dye by green seaweed *C. scalpelliformis*. From potentiometric titrations, the total organic acidity ($[COOH]_{total}$) of the green seaweed was observed to be 2.89 mmol g^{-1}. The presence of carboxylic groups and other groups were identified as components of algae structure by FT-IR analysis. The amount of dye sorbed varied with initial solution pH, dye concentration, seaweed dosage and temperature. The amount of dye uptake decreased with increase in temperature indicating that the dye biosorption is an exothermic process. At 30 °C, a maximum uptake of 27 mg of dye per gram of seaweed was exhibited by the *Caulerpa* species. The sorption data were found to follow pseudo-second order kinetics. Equilibrium data fitted well to Freundlich isotherm equation confirming the heterogeneous sorption process of basic yellow dye onto seaweed. The dye uptake process was found to be controlled by external mass transfer at earlier stages and by intraparticle diffusion at later stages. Boyd plot confirmed the external mass transfer as the slowest step involved in the sorption process. Thermodynamic parameters showed that the process is exothermic and spontaneous. The results of this work indicate that the green marine macroalga *C. scalpelliformis* constitutes a promising material for the development of a low cost biosorption technology for the removal of dyes from effluents.

Acknowledgement

One of the authors (R.A.) is grateful to Council of Scientific and Industrial Research, Government of India, New Delhi for granting Senior Research Fellowship (SRF) for his Ph.D. program.

References

[1] P. Nigam, I.M. Banat, D. Singh, R. Marchant, Microbial process for the decolorization of textile effluent containing azo, diazo and reactive dyes, Process Biochem. 31 (1996) 435–442.

[2] A. Reife, D. Betowski, H.S. Freeman, Dyes and Pigments. The Encyclopedia of Environmental Analysis and Remediation, Wiley International, New York, 1998, p. 1442.

[3] T. Robinson, G. McMullan, R. Marchant, P. Nigam, Remediation of dyes in textile effluent: a critical review on current treatment technologies with a proposed alternative, Bioresource Technol. 77 (2001) 247–255.

[4] Y. Fu, T. Viraraghavan, Fungal decolorization of dye wastewaters: a review, Bioresource Technol. 79 (2001) 251–262.

[5] Z. Aksu, Application of biosorption for the removal of organic pollutants: a review, Process Biochem. 40 (2005) 997–1026.

[6] J.Y. Wu, S.C.J. Hwang, C.T. Chen, K.C. Chen, Decolorization of azo dye in a FBR reactor using immobilized bacteria, Enzyme Microb. Technol. 37 (2005) 102–112.

[7] A. Özer, G. Akkaya, M. Turabik, Biosorption of Acid Red 274 (AR274) on *Enteromorpha prolifera* in a batch system, J. Hazard. Mater. 126 (2005) 119–127.

[8] G. Akkaya, A. Özer, Biosorption of Acid Red 274 (AR274) on *Dicranella varia*: determination of equilibrium and kinetic model parameters, Process Biochem. 40 (2005) 3559–3568.

[9] M.S. Chiou, H.Y. Li, Adsorption behavior of reactive dye in aqueous solution on chemical cross-linked chitosan beads, Chemosphere 50 (2003) 1095–1105.

[10] Y.C. Wong, Y.S. Szeto, W.H. Cheung, G. McKay, Adsorption of acid dyes on chitosan-equilibrium isotherm analyses, Process Biochem. 39 (2004) 695–704.

[11] C. Namasivayam, N. Kanchana, R.T. Yamuna, Waste banana pith as adsorbent for the removal of rhodamine-B from aqueous solutions, Waste Manage. 13 (1993) 89–95.

[12] Z. Aksu, Reactive dye bioaccumulation by *Saccharomyces cerevisiae*, Process Biochem. 38 (2003) 1437–1444.

[13] Z. Aksu, S. Tezer, Equilibrium and kinetic modelling of biosorption of Remazol Black B by *Rhizopus arrhizus* in a batch system: effect of temperature, Process Biochem. 36 (2000) 431–439.

[14] J. Swamy, J.A. Ramsay, The evaluation of white rot fungi in the decoloration of textile dyes, Enzyme Microb. Technol. 24 (1999) 130–137.

[15] B. Volesky, in: B. Volesky (Ed.), Biosorption of Heavy Metals, CRC Press, Boca Raton, FL, 1990, p. 3.

[16] N. Tewari, P. Vasudevan, B.K. Guha, Study on biosorption of Cr(VI) by *Mucor hiemalis*, Biochem. Eng. J. 23 (2005) 185–192.

[17] R. Aravindhan, B. Madhan, J.R. Rao, B.U. Nair, T. Ramasami, Bioaccumulation of chromium from tannery wastewater: an approach for chrome recovery and reuse, Environ. Sci. Technol. 38 (2004) 300–306.

[18] S.J. Allen, G. McKay, J.F. Porter, Adsorption isotherm models for basic dye adsorption by peat in single and binary component systems, J. Colloid Interf. Sci. 280 (2004) 322–333.

[19] T. Akar, T.A. Tamir, I. Kiran, A. Ozcan, A.S. Ozcan, S. Tunali, Biosorption potential of *Neurospora crassacells* for decolorization of Acid Red 57 (AR57) dye, J. Chem. Technol. Biotechnol. 81 (2006) 1100–1106.

[20] S. Lagergren, Zur theorie der sogenannten adsorption gelöster stoffe. Kungliga Svenska Vetenskapsakademiens, Handlingar 24 (1898) 1–39.

[21] Y.S. Ho, G. McKay, Pseudo-second order model for sorption processes, Process Biochem. 34 (1999) 450–465.

[22] Y.S. Ho, G. McKay, Sorption of dye from aqueous solution by peat, Chem. Eng. J. 70 (1998) 115–124.

[23] G. McKay, S.J. Allen, I.F. Mc Convey, M.S. Otterburn, Transport processes in the sorption of colored ions by peat particles, J. Colloid Interf. Sci. 80 (1981) 323–339.

[24] G. McKay, M.S. Otterburn, A.G. Sweeney, Surface mass transfer processes during colour removal from effluent using silica, Water Res. 15 (1981) 327–331.

[25] Q. Sun, L. Yang, The adsorption of basic dyes from aqueous solution on modified peat-resin particle, Water Res. 37 (2003) 1535–1544.

[26] G.E. Boyd, A.W. Adamson, L.S. Myers, The exchange adsorption of ions from aqueous solution by organic zeolites. II. Kinetics, J. Am. Chem. Soc. 69 (1947) 2836–2848.

[27] V.K. Gupta, I. Ali, Removal of DDD and DDE from wastewater using bagasse fly ash, a sugar industry waste, Water Res. 35 (2001) 33–40.
[28] H. Freundlich, Adsorption in solution, Z. Phys. Chem. 40 (1906) 1361–1368.
[29] I. Langmuir, The adsorption of gases on plane surfaces of glass, mica, and platinum, J. Am. Chem. Soc. 40 (1918) 1361–1368.
[30] M.R. Reddy, S.J. Dunn, Distribution coefficients for nickel and zinc in soils, Chem. Phys. 11 (1986) 303–313.
[31] M.P.F. Fontes, P.C. Gomes, Simultaneous competitive adsorption of heavy metals by the mineral matrix of tropical soils, Appl. Geochem. 18 (2003) 795–804.
[32] Y. Yu, Y.Y. Zhuang, Z.H. Wang, Adsorption of water-soluble dye onto functionalized resin, J. Colloid Interf. Sci. 242 (2001) 288–293.
[33] M. Dogan, M. Alkan, Removal of methyl violet from aqueous solution by perlite, J. Colloid Interf. Sci. 267 (2003) 32–41.